LETTERS

Metabolic gene regulation in a dynamically changing environment

Matthew R. Bennett[1,2]*, Wyming Lee Pang[1]*†, Natalie A. Ostroff[1], Bridget L. Baumgartner[1], Sujata Nayak[1], Lev S. Tsimring[2] & Jeff Hasty[1,2]

Natural selection dictates that cells constantly adapt to dynamically changing environments in a context-dependent manner. Gene-regulatory networks often mediate the cellular response to perturbation[1–3], and an understanding of cellular adaptation will require experimental approaches aimed at subjecting cells to a dynamic environment that mimics their natural habitat[4–9]. Here we monitor the response of *Saccharomyces cerevisiae* metabolic gene regulation to periodic changes in the external carbon source by using a microfluidic platform that allows precise, dynamic control over environmental conditions. We show that the metabolic system acts as a low-pass filter that reliably responds to a slowly changing environment, while effectively ignoring fast fluctuations. The sensitive low-frequency response was significantly faster than in predictions arising from our computational modelling, and this discrepancy was resolved by the discovery that two key galactose transcripts possess half-lives that depend on the carbon source. Finally, to explore how induction characteristics affect frequency response, we compare two *S. cerevisiae* strains and show that they have the same frequency response despite having markedly different induction properties. This suggests that although certain characteristics of the complex networks may differ when probed in a static environment, the system has been optimized for a robust response to a dynamically changing environment.

To probe the response of a metabolic gene network to a fluctuating environment, we developed a microfluidic platform that can subject a population of cells to a continuously varying supply of medium (Fig. 1). The device is designed to generate a fluctuating signal of medium by dynamically combining two medium-filled reservoirs in accordance with a time-dependent function. Feeding channels deliver the media downstream to a customizable growth chamber, which for this study was constructed to constrain a population of yeast cells to grow in a monolayer, permitting long-term data acquisition[10]. The composition of the medium is dynamically controlled by a fluidic switch[11], such that changes in the upstream source may be detected almost immediately by the cells. The fluidic switch was optimized to generate a linear range of mixing ratios from the two media inputs, allowing a variety of periodic waveforms or random signals to be generated (see Supplementary Information for full details of the device).

As a quantifiable reporter of the cellular response to environmental fluctuations, we fused the native Gal1 protein of *S. cerevisiae* to the yeast-optimized enhanced cyan fluorescent protein (yECFP)[12,13]. The enzymes for galactose utilization, including Gal1, are among the most tightly regulated proteins in yeast. Because glucose requires much less energy to metabolize, cells will consume galactose only if glucose is not available. *S. cerevisiae* has therefore evolved a highly complex regulatory network to ensure that the galactose-metabolizing enzymes will be strongly activated when they are needed, but tightly repressed if glucose is present in the environment (Fig. 2a). Because the network has been well studied and involves regulatory motifs common to many higher organisms, galactose utilization is a model for gene regulation. To build on the current understanding of its robust regulatory mechanisms, we employed our microfluidic platform to monitor the dynamics of network activation and repression in response to sinusoidal perturbations of glucose over a galactose background.

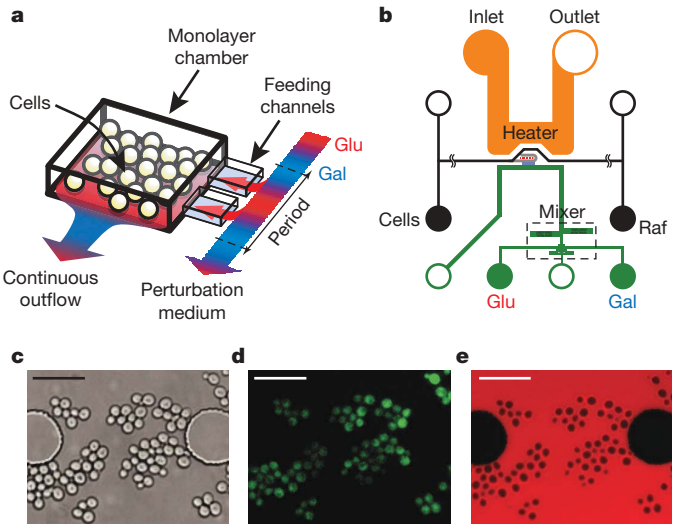

Figure 1 | Design and implementation of the microfluidic platform developed for our study. a, Conceptual design of the imaging chamber. The chamber is coupled to the switch output channel by means of multiple 'feeding' channels 1 μm tall. The feeding channels are fed by a controllable waveform generator that creates sinusoidal perturbations in the glucose concentration while maintaining constant background levels of galactose. **b**, An overview of the design showing the layout of the device. The device makes use of three flow networks for loading cells (middle, black), generating microenvironmental waveforms (bottom, green), and controlling on-chip temperature (top, orange). The imaging chamber (centre, grey region) is designed to be about 4 μm tall to constrain a population of yeast cells to grow in a monolayer. **c**, Representative bright-field image of cells growing in the imaging chamber. These images were used to measure the total size of the colony. Large circles are support posts in the chamber. Scale bar, 25 μm. **d**, Green fluorescence image of the same cells as in **c**. These images allowed us to measure the amount of Gal1 in each cell. **e**, Red fluorescence image of the chamber. The glucose medium also contained a red fluorescent dye; the intensity of the red fluorescence was therefore proportional to the amount of glucose in the chamber at any given time.

[1]Department of Bioengineering, and [2]Institute for Nonlinear Science, University of California, San Diego, La Jolla, California 92093, USA. †Present address: Institute for Systems Biology, Seattle, Washington 98103, USA.
* These authors contributed equally to this work.

©2008 Macmillan Publishers Limited. All rights reserved

A population of yeast cells was subjected to sinusoidal waves of glucose concentration over a 0.2% (w/v) galactose background, with glucose concentration varying from 0% (no repression of *GAL1* transcription) to 0.25% (full repression; see Supplementary Information for repression data). For each run we changed the frequency of the glucose signal, varying the period from 0.75 to 4.5 h, and we imaged the population for a minimum of four full cycles. Time-lapse fluorescence imaging of the cell population in the growth chamber was used to calculate the amplitude ratio and phase shift of the cellular response relative to the glucose signal. The results show a maximum response frequency of about 5.6 radians h^{-1} (1.125 h period). At this frequency, the response trace was indistinguishable from a normal step-function response, whereas at the lower frequencies the temporal fluorescence trajectories clearly oscillated in response to the signal. In this sense, the galactose system seems to function as a low-pass filter that reliably responds to a slowly changing environment, while effectively ignoring fluctuations that are too fast for the cell to mount an efficient response.

Because the sinusoidal driving of the galactose utilization network leads to complex cellular behaviour, we used computational modelling to simulate the response and to uncover key aspects of the network architecture that give rise to the observed behaviour[14]. In particular, we were interested in how the interplay of the galactose and glucose utilization networks gives rise to the observed frequency response to carbon source fluctuations. By itself, the turnover of Gal1–yECFP, due either to dilution or to active degradation (or both), leads to low-pass filtering of periodic signals. However, feedback loops inherent in gene regulatory networks can alter the response of proteins to stimuli[15]. Therefore, to simulate the effects of galactose activation and glucose repression on our experimental data, we adapted a comprehensive model of the galactose network described previously[16]. This model includes the transcription and translation of the *GAL1*, *GAL2*, *GAL3*, *GAL4* and *GAL80* genes as well as the interactions of their respective proteins with each other and with galactose (such as dimerization, transport and metabolism). Whenever possible we used parameter values either at or close to the values reported previously[16]. In addition to this galactose network model, it was necessary to model the dynamics of the glucose network. The glucose network is much more complex than that of galactose[17–19] and models for it are much less well established. We therefore chose to model the glucose network with a simplified module describing a basic transport regulatory system. In it, protein products of the glucose network are responsible for transporting external glucose into the cell while internalized glucose acts to induce transcription in the network, giving rise to a positive feedback loop (see Fig. 2a).

Calibration of the computational model to the experimental data led to several important observations that would not have arisen from an analysis of steady-state batch culture data. The large amplitude ratios observed at low frequencies suggested that when glucose was added to the system the degradation rates of some galactose network components were greater than in the absence of glucose. Previous studies have suggested that components of the glucose network can actively degrade messenger RNA produced by genes involved in the galactose/glucose switch[8], and this phenomenon has also been shown to exist for the mRNA of other genes[20–22]. We therefore added enzymatic decay terms (governed by Michaelis–Menten dynamics) to the equations describing the dynamics of the *GAL1* and *GAL3* mRNA and found that it greatly increased the accuracy of the model. These two genes are among those in the galactose network that are targeted by the glucose-induced protein Mig1, which represses transcription by binding to upstream regulatory sites[19]. Thus, if proteins from the glucose network do actively degrade galactose network transcripts, *GAL1* and *GAL3* are likely targets. To test this prediction, we measured the degradation rates of *GAL1* and *GAL3* in both galactose and glucose. Both transcripts showed a 2–8-fold increase in their decay rates in the presence of glucose (see Fig. 2b and Supplementary Information), which is consistent with the values predicted by the computational model. This form of post-transcriptional regulation, in which glucose acts to downregulate Gal protein synthesis, is a previously unknown source of regulation in the galactose utilization network. Furthermore, the inclusion of glucose-mediated mRNA decay results in a model that accurately reproduces the dynamic response of a population of cells to sinusoidal repression over a large range of frequencies (Fig. 3).

Batch-culture induction characteristics for metabolic genes can vary from strain to strain or depend sensitively on the growth state of the culture. We were therefore also interested in using the model to determine how galactose induction differences would affect the response to the glucose fluctuations. The model demonstrated that

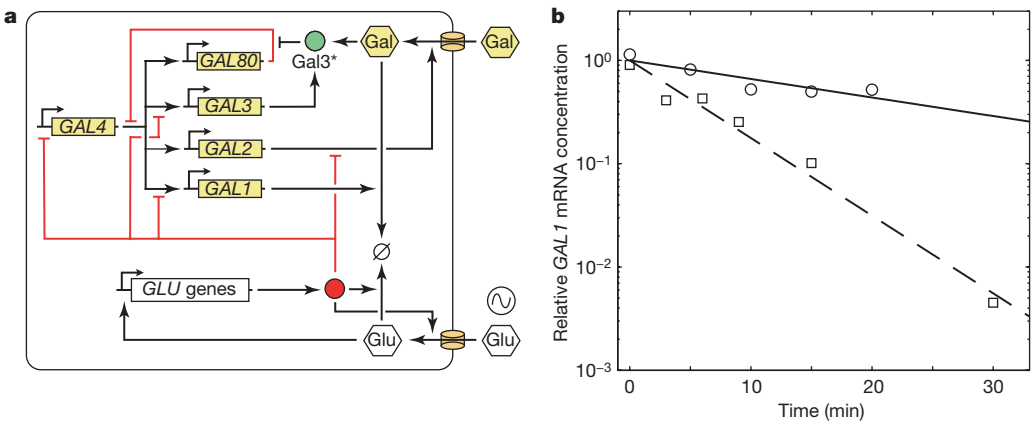

Figure 2 | Regulation in the galactose utilization network. a, Diagram of the gene regulatory networks involved. The regulatory genes in the galactose network are activated by the Gal4 protein, which binds to upstream activation sites. The *GAL80* gene provides negative feedback in the system by prohibiting the inducing affects of Gal4. Positive feedback is provided by both *GAL2* and *GAL3*. Internalized galactose can bind to Gal3, and the resulting complex binds to Gal80. Gal80 bound to the Gal3–galactose complex is incapable of repressing Gal4. In addition, the transporter Gal2 increases the amount of internal galactose, which stimulates the galactose network. The glucose network inhibits the transport of galactose and represses transcription of the galactose network in the presence of glucose through the action of Mig1, which can bind to upstream regulatory sites of *GAL1*, *GAL3* and *GAL4* (ref. 19). The glucose network also regulates the hexose transporter genes (*HXT*), responsible for transporting glucose into the cell[27], which then activates the glucose network. **b**, Experimentally measured decay of *GAL1* transcripts in galactose (circles) and glucose (squares). Also shown are the best-fit lines corresponding to half-lives of about 17 min in galactose (solid line) and 4 min in glucose (dashed line), which are similar to the values predicted by the numerical model. Data are normalized to the initial concentration of mRNA predicted by the best-fit lines. Similar results for *GAL3* transcripts are shown in Supplementary Information.

©2008 Macmillan Publishers Limited. All rights reserved

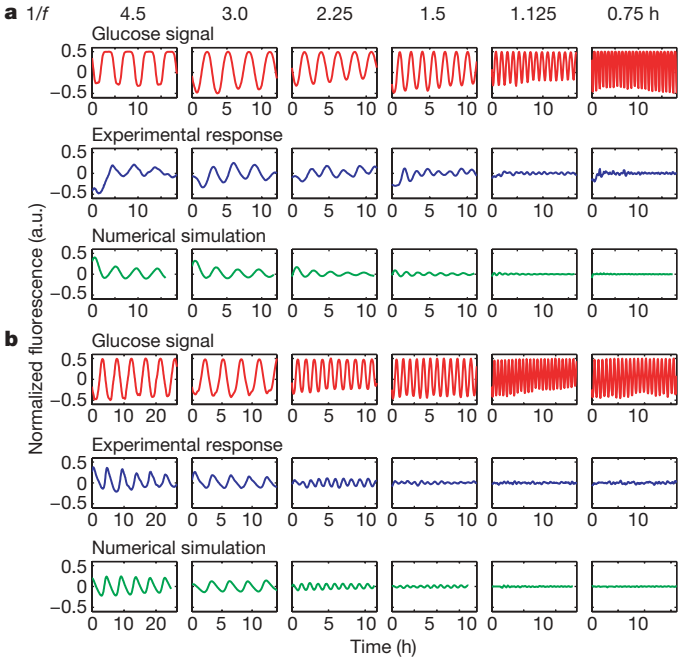

Figure 3 | Experimental and computational results for cells of two yeast strains expressing a *GAL1–yECFP* fusion gene in response to alternating glucose and galactose media. **a**, Strain K699; **b**, strain YPH499. The top row for each strain depicts the input glucose signal that was measured during each experimental run and was also used to simulate the responses. The mean fluorescence of a red tracer dye, representing the glucose concentration in the medium, is normalized and subtracted from 1 to represent the 'induction' signal used in the experimental and computational runs above. The middle rows show normalized and detrended fluorescence trajectories for a population of cells as they respond to glucose waves of various frequencies over a galactose background. In the absence of glucose, galactose induces the transcription of *GAL1–yECFP*, causing an increase in cellular fluorescence. However, as glucose is introduced into the extracellular environment, transcription of the galactose enzymes is shut off, causing a decrease in fluorescence signal as the Gal1–yECFP protein is degraded. Oscillation periods are (from left to right) 4.5, 3.0, 2.25, 1.5, 1.125 and 0.75 h. For input waves with a period shorter than 1.125 h, cells no longer responded to sinusoidal repression in a periodic fashion, demonstrating their ability to 'filter' out high-frequency environmental fluctuations. The bottom rows show simulation results for the same frequencies as above. The model, calibrated to experimental induction and repression data, accurately reproduces the cellular responses over a large range of frequencies.

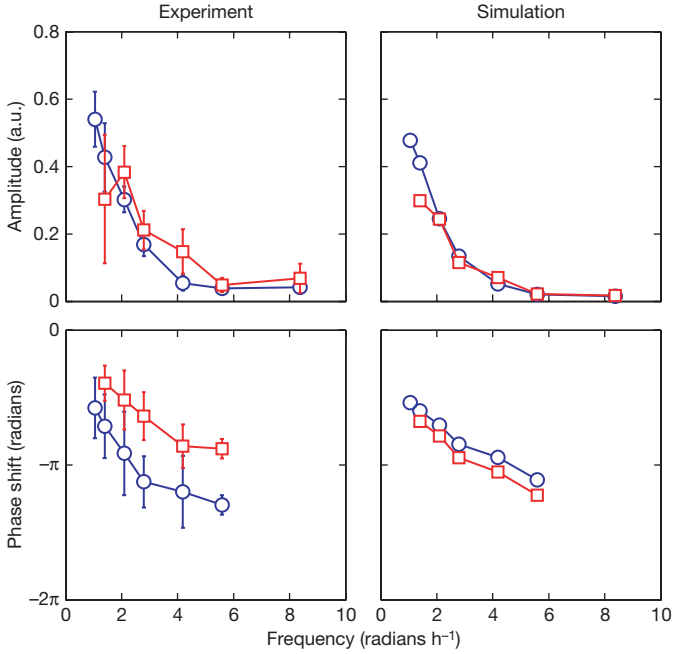

Figure 4 | Experimental and computational comparison of two yeast strains. The amplitude (top row) and phase shift (bottom row) of the response of cells to sinusoidal repression at various frequencies are shown for both K699 (red) and YPH499 (blue) strains (error bars represent s.d.). Strain YPH499 is known to have a deficiency in the galactose utilization network. For the highest-frequency trial, reliable phases could not be calculated because of noise; these results have been omitted from the graphs. The experimental data (left column) show that the amplitude responses of the two strains are strikingly similar, especially considering their significantly different induction curves (see Supplementary Information). This phenomenon was predicted by model simulations, because slight modifications to the model parameters that affected the induction and repression curves did not affect the cell population's robust response to a dynamic environment. This suggests that the complex structure of the glucose and galactose networks may confer robustness on cells even if faced with seemingly detrimental network deficiencies. The phase responses (bottom row) of the two strains showed a marked difference, with YPH499 cells having a greater phase lag than K699 cells.

significantly different galactose induction does not necessarily lead to significant differences in the response characteristics (data not shown). In other words, the model led to the hypothesis that deficiencies in network induction capabilities might not hinder a cell's ability to adapt and thrive in a changing environment. The yeast strain used to collect the present data, K699, is sensitive to external galactose concentrations, with full induction of the galactose network occurring at about 0.05% (w/v) galactose. To test our hypothesis, we turned to a strain (YPH499) that is known to have a deficiency in the galactose utilization network that causes it to require more galactose than 'normal' to induce production of the galactose enzymes[23]. YPH499 is a derivative of a *GAL2* mutant strain, and although the mutations were reportedly repaired, the *GAL2* alleles in many of the derivative strains have been shown to cause significantly impaired galactose uptake[23]. Gal2 protein is responsible for the transport of extracellular galactose into the cell and its activity is markedly different in YPH499 from that in K699. Our flow cytometry population data demonstrated that YPH499 cells require about tenfold more galactose than K699 cells to reach full induction (see Supplementary Information).

Despite the difference in induction sensitivity between K699 and YPH499 cells, our model predicted that inefficient Gal2 transport does not translate into a less robust response to a fluctuating environment. This suggests that the complex interplay of the glucose and galactose networks may confer robustness on cells even if faced with deficiencies in the induction characteristics. To validate this finding, we repeated the microfluidic runs at each frequency, this time using the YPH499 strain with a Gal1–yECFP fusion. As predicted, the amplitude responses of the two strains are strikingly similar (Fig. 4), especially considering the significant difference in their galactose sensitivity. We do not at present know the underlying mechanistic property of the regulatory network that leads to the robust response of the two strains. Future studies might endeavour to deduce this mechanism through the systematic deconstruction of the regulatory elements in a single strain. Although the present study shows how robustness can occur despite large differences in induction characteristics, one could further investigate the generality of this phenomenon by comparing the responses of many different strains to different types of temporal perturbation.

METHODS SUMMARY

Dynamic environment experiments. Cells containing a *GAL1–yECFP* fusion were imaged every 5 min for up to 24 h by using time-lapse fluorescent microscopy to estimate the concentration of Gal1 as a function of time. Cells were constrained to grow in a custom-designed microfluidic platform that permitted the dynamically controlled mixing of two growth media. Our inducing medium contained

©2008 Macmillan Publishers Limited. All rights reserved

2% raffinose and 0.2% galactose, whereas the repressing medium contained 2% raffinose, 0.2% galactose and 0.25% glucose. The resulting images were processed with cell segmentation and tracking software, and the population-averaged fluorescence concentrations were measured. To ensure correct waveform generation, glucose concentrations were monitored by introducing a red fluorescent tracer dye (sulphorhodamine 101, 0.01 mg ml^{-1}) to the repressing medium.

Microfluidic chips and waveform generation. The polydimethylsiloxane microfluidic devices were designed to permit the monolayer growth of yeast cells in the imaging chamber and were fabricated with standard replica-moulding techniques[24–26]. An upstream fluidic switch controlled the input of medium into the chamber by mixing the flows of the inducing and repressing media. The mixing ratio of the two media was governed by a software-controlled, custom-designed pressurization system that was able to produce time-varying waveforms consistently.

mRNA degradation experiments. The degradation rates of *GAL1* and *GAL3* transcripts were measured with standard reverse-transcriptase-mediated quantitative polymerase chain reaction techniques. Knockout strains for both genes were first created, and then ectopic *GAL1* and *GAL3* were placed back into the cell under the control of a doxycycline-repressible promoter. Half-lives of mRNAs were measured from cells grown in the presence or absence of glucose.

Complete details of all materials and methods used and the specifics of the computational model are available in Supplementary Information.

Received 14 April; accepted 25 June 2008.
Published online 30 July 2008.

1. Beadle, G. W. & Tatum, E. L. Genetic control of biochemical reactions in *Neurospora. Proc. Natl Acad. Sci. USA* **27,** 499–506 (1941).
2. Jacob, F. & Monod, J. Genetic regulatory mechanisms in the synthesis of proteins. *J. Mol. Biol.* **3,** 318–356 (1961).
3. Douglas, H. C. & Hawthorne, D. C. Regulation of genes controlling synthesis of the galactose pathway enzymes in yeast. *Genetics* **54,** 911–916 (1966).
4. Thattai, M. & Shraiman, B. I. Metabolic switching in the sugar phosphotransferase system of *Escherichia coli. Biophys. J.* **85,** 744–754 (2003).
5. Lipan, O. & Wong, W. H. The use of oscillatory signals in the study of genetic networks. *Proc. Natl Acad. Sci. USA* **102,** 7063–7068 (2005).
6. Kussell, E. & Leibler, S. Phenotypic diversity, population growth, and information in fluctuating environments. *Science* **309,** 2075–2078 (2005).
7. Kruse, K. & Julicher, F. Oscillations in cell biology. *Curr. Opin. Cell Biol.* **17,** 20–26 (2005).
8. Ronen, M. & Botstein, D. Transcriptional response of steady-state yeast cultures to transient perturbations in carbon source. *Proc. Natl Acad. Sci. USA* **103,** 389–394 (2006).
9. Thattai, M. & van Oudenaarden, A. Stochastic gene expression in fluctuating environments. *Genetics* **167,** 523–530 (2004).
10. Cookson, S., Ostroff, N., Pang, W. L., Volfson, D. & Hasty, J. Monitoring dynamics of single-cell gene expression over multiple cell cycles. *Mol. Syst. Biol.* **1,** doi:10.1038/msb4100032 (2005).
11. Groisman, A. *et al.* A microfluidic chemostat for experiments with bacterial and yeast cells. *Nature Methods* **2,** 685–689 (2005).
12. Sheff, M. A. & Thorn, K. S. Optimized cassettes for fluorescent protein tagging in *Saccharomyces cerevisiae. Yeast* **21,** 661–670 (2004).
13. Raser, J. M. & O'Shea, E. K. Control of stochasticity in eukaryotic gene expression. *Science* **304,** 1811–1814 (2004).
14. Hasty, J., McMillen, D., Isaacs, F. & Collins, J. J. Computational studies of gene regulatory networks: *in numero* molecular biology. *Nature Rev. Genet.* **2,** 268–279 (2001).
15. Savageau, M. A. Comparison of classical and autogenous systems of regulation in inducible operons. *Nature* **252,** 546–549 (1974).
16. de Atauri, P., Orrell, D., Ramsey, S. & Bolouri, H. Evolution of 'design' principles in biochemical networks. *Syst. Biol.* **1,** 28–40 (2004).
17. Demir, O. & Kurnaz, I. A. An integrated model of glucose and galactose metabolism regulated by the *GAL* genetic switch. *Comput. Biol. Chem.* **30,** 179–192 (2006).
18. Kaniak, A., Xue, Z., Macool, D., Kim, J. & Johnston, M. Regulatory network connecting two glucose signal transduction pathways in *Saccharomyces cerevisiae. Eukaryot. Cell* **3,** 221–231 (2004).
19. Verma, M., Bhat, O. J. & Venkatesh, K. V. Steady-state analysis of glucose repression reveals hierarchical expression of proteins under Mig1p control in *Saccharomyces cerevisiae. Biochem. J.* **388,** 843–849 (2005).
20. Scheffler, I. E., de la Cruz, B. J. & Preito, S. Control of mRNA turnover as a mechanism of glucose repression in *Saccharomyces cerevisiae. Biochem. Cell Biol.* **30,** 1175–1193 (1998).
21. de la Cruz, B. J., Prieto, S. & Scheffler, I. E. The role of the 5′ untranslated region (UTR) in glucose-dependent mRNA decay. *Yeast* **19,** 887–902 (2002).
22. Andrade, R. P., Kötter, P., Entian, K. D. & Casal, M. Multiple transcripts regulate glucose-triggered mRNA decay of the lactate transporter *JEN1* from *Saccharomyces cerevisiae. Biochem. Biophys. Res. Commun.* **332,** 254–262 (2005).
23. Rohde, J. R., Trinh, J. & Sadowski, I. Multiple signals regulate *GAL* transcription in yeast. *Mol. Cell. Biol.* **20,** 38803886 (2000).
24. Whitesides, G. M., Ostuni, E., Takayama, S., Jiang, X. Y. & Ingber, D. E. Soft lithography in biology and biochemistry. *Annu. Rev. Biomed. Eng.* **3,** 335–373 (2001).
25. Whitesides, G. M. *et al.* Soft lithography and bioanalysis. *Abstr. Pap. Am. Chem. Soc.* **227,** U113–U113 (2004).
26. Xia, Y. & Whitesides, G. M. Soft lithography. *Angew. Chem. Int. Edn Engl.* **37,** 550–575 (1998).
27. Boles, E. & Hollenberg, C. P. The molecular genetics of hexose transport in yeasts. *FEMS Microbiol. Rev.* **21,** 85–111 (1997).

Supplementary Information is linked to the online version of the paper at www.nature.com/nature.

Acknowledgements We thank A. Groisman for useful discussions regarding microfluidic design; D. Volfson and C. Grilly for aid in development and testing of image segmentation and tracking algorithms, and M. Ferry for his suggestions on microbiology. This work was supported by the National Institute of General Medical Sciences of the National Institutes of Health.

Author Information Reprints and permissions information is available at www.nature.com/reprints. Correspondence and requests for materials should be addressed to J.H. (hasty@ucsd.edu).

©2008 Macmillan Publishers Limited. All rights reserved